

# Some applications of virtual instrumentation in NDT

G. D'Ans, P. Ripak, P. Cerckel, D. Degrève and M. Katz

*Laborelec, St Genesius Rode, Belgium*

P. Fontana, A. Xheneumont and F. Vanseven

*Applied Mechanics Department, Free University of Brussels, Brussels, Belgium*

**ABSTRACT:** Several NDT applications were developed as virtual instruments (vi in short) using Labview. This greatly shortened the prototyping phase, while tailoring the man-machine interface to end users' specs. Labview provides numerous reliable data processing modules. It also supports versatile drivers for multifunction data acquisition cards. Such tools lead to advanced custom-made vi's addressing applications running on inexpensive PCs and hitherto reserved to dedicated devices. Transportable PCs loaded with multiple vi's become an interesting platform for tests and measurements in the field upon short notice. Several NDT applications are detailed: (a) a mini-expert to diagnose faults in rolling-element bearings (b) a vi for time-frequency analyses of gear drives (c) monitoring and diagnosing shaft vibrations (d) a vi to streamline the analysis of wear in fuel rods for nuclear power plants.

## 1 INTRODUCTION

Test and measurements dealing with power generation, power transmission as well as the application of electricity represent of the most important missions of Laborelec, the Belgian Laboratory of the Electricity Industry [1]

Special measurement schemes often require customized data processing and man-machine interfaces. They are most profitable in field applications at the customers' plants. Thus mobility is at a premium. Since feedback from the site often suggest further tuning of the methods developed in a laboratory. Thus some high versatility in development techniques help further tuning them, as is already the case when developing the method on test rigs.

Labview G programming [2] combined with powerful transportable PCs [3] fitted with fast and versatile data acquisition cards provide an interesting approach.

### 1.1 *Reducing developments and increasing the dialogue*

Key to reducing time-to-market developments is to ensure a good interface between the end users, the specialists of the application and computer specialists. Labview Graphical programming allows specialists and end users to prototype their applications fast. Only when computer and programming issues

arise will they turn to the computer specialists. The latter then may finalize the final package knowing the architecture of the application. Nice thing about G programming is the availability of a (2-dimensional) flow chart encapsulating the expertise. This eases communication forcing the application specialist to well define the expertise and have a medium to discuss its features. In other words, G programming provides a common platform for parallel engineering.

### 1.2 *The NDT applications*

Amongst the following NDT applications, some were almost entirely developed by freshly graduated mechanical engineers from the free University of Brussels [4] without any special programming background. These are:

- A mini-expert for rolling-element bearings
- A time-frequency analyzer for the vibro-acoustic diagnosis of gear box defects
- A mini-monitoring of shaft vibrations for rotating machinery

All these application rely on a common data acquisition card. Fitting a transportable PC with it supplies field engineers with all those applications at once. This saves them the hassle to carry cargoes of dedicated devices to address possibly unexpected troubleshooting applications in the field.

The RCCA application is a virtual instrument easing the analysts' task without its own G-based data acquisition module.

## 2 ROLLING-ELEMENT BEARING MINI-EXPERT

### 2.1 Purpose

Detect surface defects in anti-friction bearings such as on rollers (balls), inner and outer races using standard outboard accelerometers. Increase the detection capabilities while avoiding false alarms.

### 2.2 Background information

When rolling elements pass on a surface defect (spall), they generate families of shock elastic waves that are picked up by the outboard accelerometer some distance away from the source.

- The rates of occurrences of these waves are BPFI, BPFO, or 2 X BSF depending on the respective locations of a spall: IR (inner race) OR (outer race) or roller. The rotational speed of the shaft. Their amplitude can be modulated at the rate of the spall passages through the load zone: none for BPFO, rpm period for BPFI and FTF(cage rotational frequency) for BSF.
- All these frequencies are proportional to the shaft rpm
- All these frequencies depend on the bearing dimension that can be retrieved from the bearing nomenclature.[5,6]

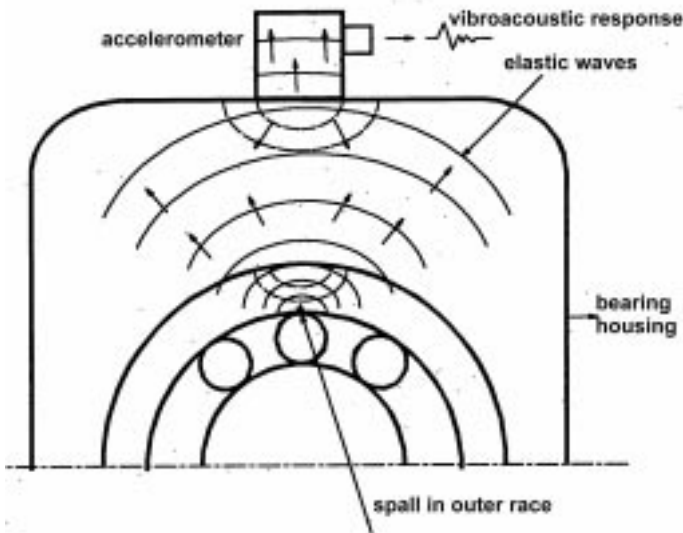


Fig.1 General measurement setup with standard accelerometer used for vibration monitoring.

### 2.3 Typical defect signatures in the time domain

**Outer race defect:** Succession of shocks with about the same amplitude whose spacing is the period inverse of B(all)P(assing)F(requency)O(uter) race characteristic frequency of the bearing. Rotational speed is 1500 rpm in this example obtained with a calibrated defect on the outer race of a SKF22NU15EC. Vibro-acoustic responses are digitally high-pass filtered from 2 kHz on. No modula-

tion.

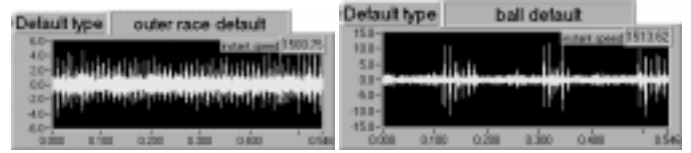


Fig.2. Typical vibro-acoustic responses of inner race and roller defects in a SKFNU2215EC at ca 1500 rpm.

**Roller (roller)surface defect:** Same remark as before except that shock spacing corresponds to twice the characteristic B(all)S(pin)F(requency) and is modulated with a period corresponding to one cage rev.

### 2.4 Expert system as a LABVIEW vi: Basic idea behind data processing

Suppose that a surface defect appears at the surface of a ball (roller) as shown below.

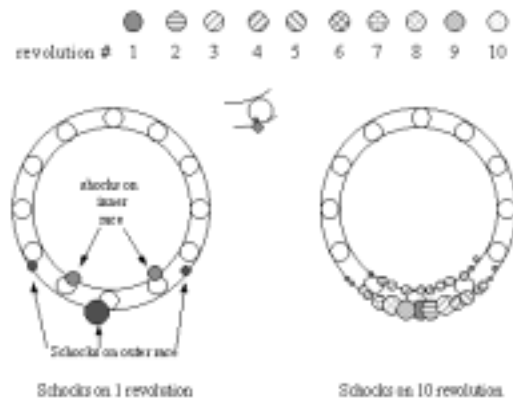


Fig.3. Pseudo echoes as generated by a ball defect on a SKF.

This defect causes successive shocks as it alternately bumps into the inner and the outer race. For a vertical, such shocks tend to increase with the pressure between roller and races. This pressure reaches a maximum when roller motion reaches the lowest point. On either side of this position, shocks amplitudes decrease. They even disappear when the roller in the upper half of its motion.

Black and gray circles indicate the positions of shock occurrences with the outer and inner races, respectively.

Circle radii are proportional to shock intensities whose distribution depends on the profile of the load zone. Shock waves from the inner race may be more attenuated than would be the case from the outer race, due to a longer travel path to the outboard accelerometer. Thus gray circles are smaller.

The right-hand side bearing shows the position of contacts of the defects with the races over several successive cage revs.

Let the largest black circle act as the source an incident acoustic wave. Then consider that subsequent gray and black circles are pseudo echoes. They are not due to the propagation of acoustic shock waves but rather to the dynamics and kinematics of bearings.

Attenuated echo-like shock waves lend themselves to cepstral techniques when one wishes to separate them from the main incident shock wave and reach a high data compression ratio. To this aim, one must exert some care to obtain sound cepstra [7]. One must indeed center the buffer of data within a load cycle and windowing it for proper cepstral analyses without aliasing.

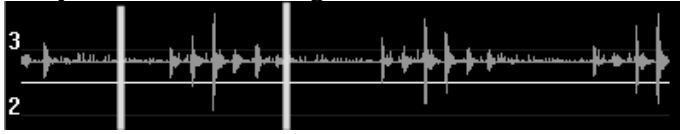


Fig.4. Automatic selection of a vibro-acoustic response of the bearing signature centered on a load zone.

Centering of the defect signature requires several steps:

- Acquire a larger data buffer to encompass the motion of the defect through several load zones
- Filter the signal to eliminate lower frequencies caused by vibrations
- Based on the distribution of this filtered signal, select a buffer whose length corresponds the half the period of a gear rev.
- Apply to it a centered double exponential window  $w(t)$  simulating an attenuation of shock waves when departing from the window center. This forces outer race defects lacking specific load zones to generate attenuated echoes fit for cepstral analyses.
- Perform the cepstral analysis

## 2.5 The mini-expert virtual instrument

It was developed in record time in Labview using all data processing modules and tested with a full-scale test rig simulating bearing defects.

Its front panel is shown below.

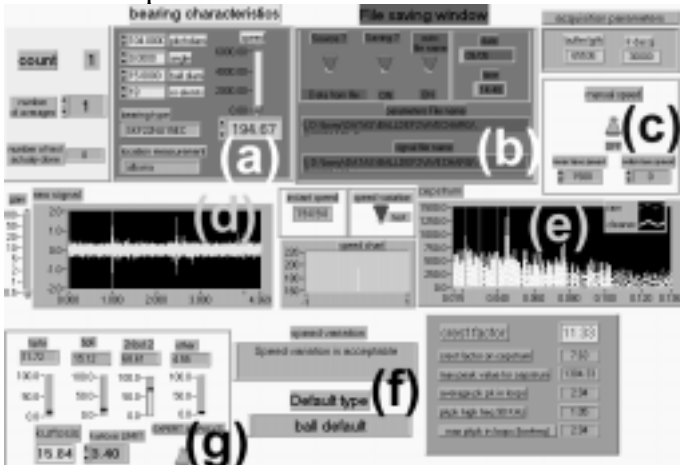


Fig.5. The user front panel of the bearing mini-expert is divided as follows:

- A description of the bearing with its type from the nomenclature and corresponding characteristics like pitch and roller (ball) diameters, number of rollers, contact angle to be entered by the user. It also displays the shaft rpm.
- A panel to control loading signatures to retrieving from a database with date and time of measurement.
- A control to select rpm from a velocity pickup or manu-

ally

- A display of the raw signature.
- A display of the power cepstra zoomed in the time interval including the periods of the bearing characteristic defects and multiples thereof (rhamonics)
- The diagnosis panel with messages: *no default, default on inner or outer races, on rollers, no shock no diagnosis.*
- A panel showing the pseudo probabilities of the different defects

## 2.6 Benchmarking

The example shows that the mini-expert spots a roller defect at very low rpm (196 rpm). Experience shows that to hold true down to less than 60 rpm, where other commercial approaches fail to diagnose a bearing fault.

## 3 DIAGNOSING GEAR MALFUNCTIONS WITH TIME-FREQUENCY ANALYSES

### 3.1 Purpose

From the vibro-acoustic response of the gear measured from outboard accelerometers, diagnose surface defects in tooth profiles and other malfunction such as pinion eccentricities, helix errors, uneven pitches, etc.

### 3.2 Measurement characteristics

Basically, one over-samples the accelerometer response at very high rates simultaneously with pulses generated once per rev by two meshing pinions (phase references).

From the response, one extracts a portion starting when a given pair of teeth meshes (in a vernier-like approach) and ending when all tooth combinations have been swept through (i.e. when top count from the smaller pinion equals the number of teeth of the bigger one). One then reduces it by a decimation scheme with variable time pitch driven by the occurrence times of the tops generated by the faster pinion. Basically one extracts a fixed number of samples between two successive top occurrences. If the speed does not vary much over one rev, this amounts to sample responses at equally spaced angular positions of the pinions.

Decimated buffers are ideal for

- order tracking with a proper indexing of the pairs of meshing profiles
- period averaging of successive sequences of meshing combinations since the buffers are phase-locked and with the same length. This reduces the contributions to the vibro-acoustic response that are not synchronous with the pinion revs.

When feasible in practice, linear encoders

mounted on one shaft could generate an external for data acquisition.

### 3.3 Example of measurement setup

For a 41:37 gear drive one can specify that the decimation produce 40 samples per mesh. In this case, one ends up with buffers holding  $41 \times 37 \times 40 = 60680$  samples. For a proper variable time-pitch decimation, the initial buffer must be over-sampled with an at least a 3:1 ratio. Let the smaller pinion rotate at 1200 rpm. The rate of data acquisition is at least  $37 \times 40 \times 20 \times 3 = 88800$  samples/sec. The buffer length must at least cover two complete meshing sequences, i.e.  $41 \times 37 \times 40 \times 3 \times 2 = 364080$  samples. Since the two tops from each pinion are also full-fledged data acquisition channels, the total count for data acquisition rate and buffer length become:

Buffer length:  $3 \times 364080 = 1092240$  samples

Aggregate acquisition rate:  $3 \times 88800 = 266400$  samples/sec.

### 3.4 Computer hardware issues

From the above example, one must clearly use fast ADC cards with DMA transfers. RAM space slowly becomes an issue, because subsequent data processing requires casting the buffers in double format. Hence a buffer length amounts to ca 9 Mbytes. Thus PC with large amount of RAM are required for this type of data acquisition.

In order to generate the time-frequency spectrograms mentioned below, one performs the converse of a data reduction. As a result, one must fit PCs with sizable RAM sizes to avoid swapping and perform the analysis with some comfort. A PII 400 MHz with 256 Mbytes RAM perform well in this application.

### 3.5 Time-frequency gear diagnosis

There is a J(oint)T(ime)F(requency)A(nalysis) or JTFA toolkit[2, 9, 10] in Labview. It allows performing vibro-acoustic time-frequency analyses to the decimated buffer. One must rather talk about a time/order track analysis instead to the nature of the buffer. It follows that no frequency due to rpm variations will cause frequency modulations in the spectrograms below.

### 3.6 Test rig

A special rig allows testing damaged gears with calibrated defect with variable torque and speeds.

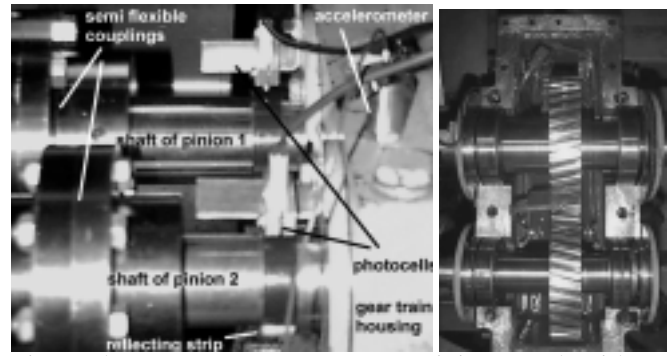


Fig.6. The measurement setup: two pinions, each with a reflecting strip and matching photocell to synchronize the data acquisition buffer to start with the same tooth profiles meshing. The type of helical gear tested (5mm module, 200 mm shaft spacing), 41:37 transmission ratio. An outboard standard accelerometer picks up the vibro-acoustic response of the gear train.

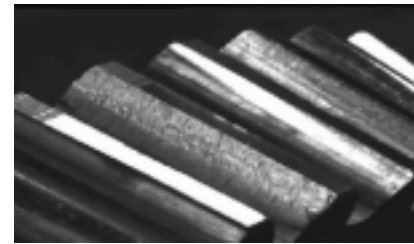


Fig.7. One pinion with two successive tooth profiles damaged. The second pinion with only one profile damaged.

### 3.7 The analysis virtual instrument

The front panel is shown below. Another vi deals with the phase-locked data acquisition

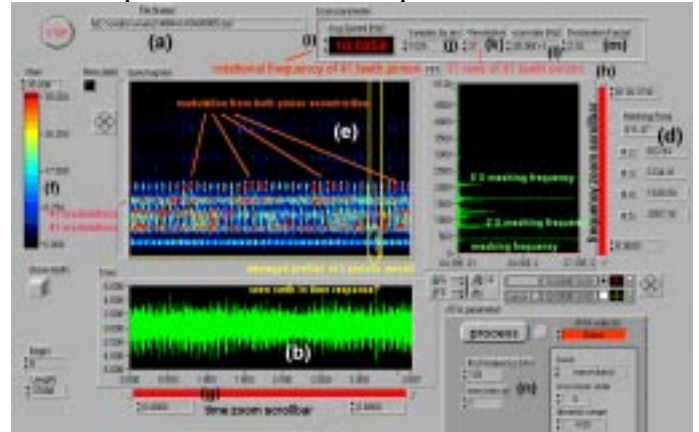


Fig.8. Front panel of the vi for the time-frequency analysis of gear train vibro-acoustic signatures:

- (a) Input file for analysis
- (b) Signal from the accelerometer
- (c) Fourier transform of the accelerometer signature with
- (d) Indicators for the meshing frequency and its harmonics
- (e) Time frequency spectrogram (Labview intensity graph) with
- (f) Color intensity scale for the spectrogram
- (g) Scrollbar for time zoom
- (h) Scrollbar for frequency zoom
- (i) Rotational frequency of the largest pinion
- (j) Number of samples per rev of largest pinion
- (k) Number of revs of largest pinion for data acquisition buffer
- (l) Data over-sampling frequency
- (m) Decimation factor
- (n) Selection of type of JTFA analysis (here Gabor narrow-band)

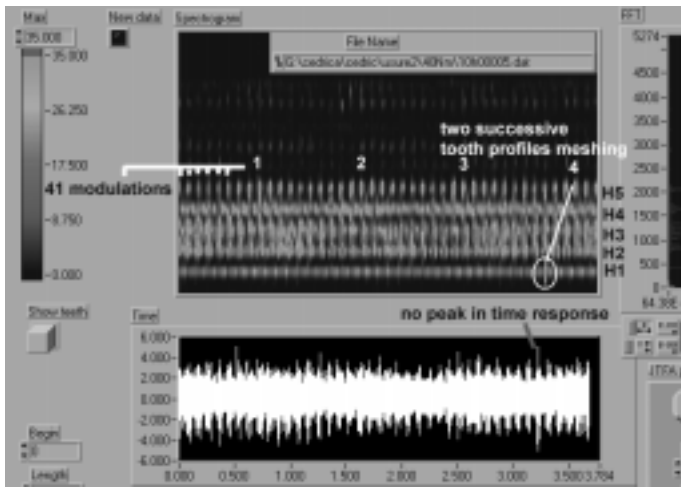


Fig.9. Close-up of the previous front panel with the Gabor spectrogram over 37 successive revs of the 41 teeth pinion. On notices:

- 41 amplitude modulations at the meshing frequency (H1) and its harmonics H2 to H5. Higher harmonics are filtered out from 3000 Hz on.
- A single amplitude burst at H1 corresponding to the damaged tooth profiles meshing
- No corresponding peak in the time response
- A 4-fold amplitude modulation at H5 ( 1 2 3 4 )

From the above close-up of the vi panel, one concludes that:

- The smaller pinion exhibits either some eccentricity and/or lack of perpendicularity to the shaft (improper mounting)
- The Gabor spectrogram detects the damage in the tooth profile.
- The time signal does not!
- Some smaller eccentricity of the larger 41 teeth pinion combines with the stronger one of the smaller 37-teeth pinion to produce a cross amplitude modulation 4 times over the whole meshing cycle
- No pitch error besides that of the damaged profile shows up. The gears were cut properly.

This example demonstrates the power of time-frequency analyses in diagnosing failures of tooth profiles.

## 4 SHAFT VIBRATIONS

### 4.1 Purpose

Diagnose malfunctions in shaft lines of rotating machinery like unbalances, rubs, cracks, proximity to resonances, etc. Provide vibration measurements to perform balancing. Compare vibration levels to standard vibration norms for rotating machinery

### 4.2 Background

Sensors are either proximity eddy probes for shaft vibrations or eccentricities or seismic sensors. Vi-

brations are expressed in rms velocity or displacement. This requires integration of the signal from seismic sensors.

Typically, one restricts the analysis to the 10-1000 Hz ranger for vibrations. Thus data acquisition rates are lower than for the previous vibro-acoustic applications. Due to a higher channel count, the aggregate data acquisition rises again.

Real-time performance is more an issue in this application. During startups and coast-downs of machines Trending may not miss transients of vibrations. This requires fast processors, but with less memory than in gear analyses where real time is less important.

Analyses are of several types:

- Trends of vibration overall levels
- Order track
- Vector monitoring
- Cascaded spectra or, more efficient in display usage, intensity charts
- Full spectra to detect forward and backward whirl with eddy probes and shaft vibrations
- Etc.

Data acquisition is somewhat simpler than for gear analyses. Once again,

- the shaft is fitted with a phase reference that triggers the data acquisition
- Over-sampling occurs over successive revs
- Variable time-pitch decimation reduces buffers to produced vibration sampled at equally spaced angular interval of the shaft revolution over a power 2 number of revs. This protects further FFTs from leakage
- Low-pass multi-channel filters prevents aliasing
- Simple and/or double integration of signals form seismic sensors to tailor them for vibration norms
- Rotational speed tracking zero phase shift high-pass filters applied to decimated buffers
- Etc.

Labview includes most tools to carry out the above tasks and validate the algorithms. It also provides versatile data acquisition cards (MIO) with flexible, user-friendly and reliable drivers.

As a result, one could set up a tool for vibration analyses in record time.

### 4.3 Some vi panels for the vibration package for rotating machinery.

#### 4.3.1 Vector monitoring

The partial vi panel below shows how the package performs vector monitoring of shaft vibration when crossing a critical speed for 2 vibration channels. Such features are useful to diagnose unbalances and perform a subsequent shaft balancing.

## 5 ROD CLUSTER CONTROL ASSEMBLY (RCCA) INSPECTIONS [12]

### 5.1 Purpose

The functions of RCCA rod are:

- Regulation of the neutron flux in the nuclear reactor
- Safety shutdown of the reactor

There are ca 32 to 52 such assemblies in a typical reactor. Due to operational vibrations within their respective guides, individual rods can undergo some damages such as:

- Wear (guide cards, continuous guide)
- Tip swelling
- long./circ. Cracking

Due to different configuration of the rod guides at different heights, wear can basically exhibit several shapes. The analysis aims at identifying their shape or nature and their severities.

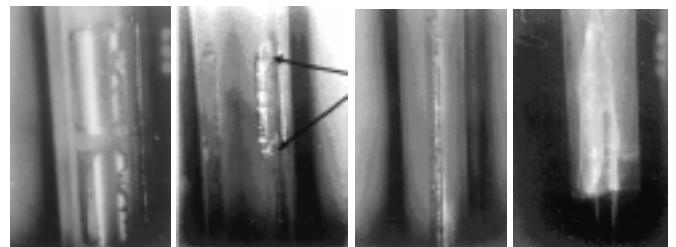


Fig.12. Different types of rod wear: circular, longitudinal (migrating material), continuous guide and rod tip.

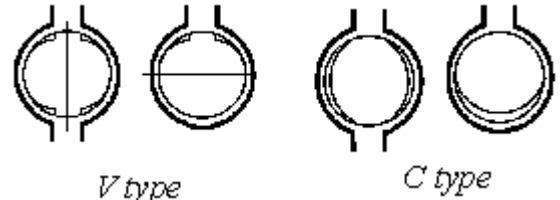


Fig.13. Types of rod wear depending on guide geometry.

Growing rod damages increase the following risks:

- poor RCCA insertion in fuel assembly,
- Break of rod(s)
- Loss of neutron absorber in reactor.

Regular inspections of the integrity of rods are thus mandatory.

### 5.2 Measurement layout

Multiple rods are lowered spider-like through an inspection block with matched penetrations fitted each with a special aggregate sensor consisting of 9 eddy current probes:

- 8 local probes measuring the local wear at 45° intervals
- 1 integrating probe.

From the responses of the distributed probes, one identifies the shape of the defect. The integrating probes monitor the structural integrity of the rod.

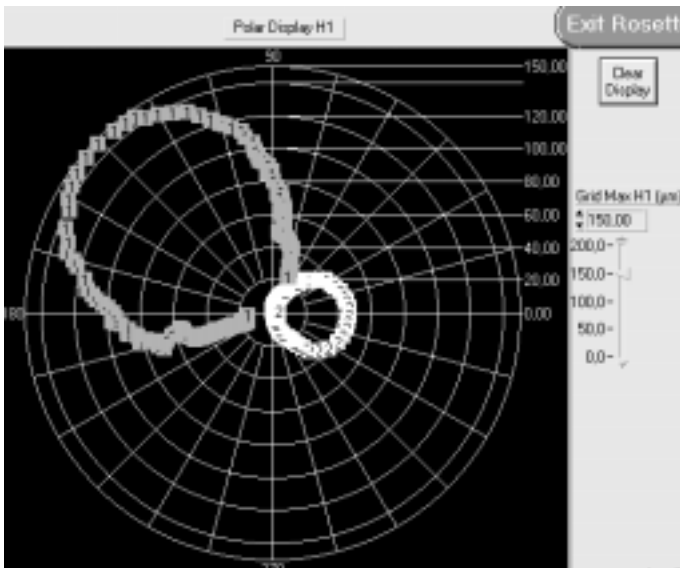


Fig.10. Running-speed vibration vectors through critical speeds. One can visualize the vibration vectors for other harmonics in another polar display. Full scale is 150  $\mu$  for eddy probes.

### 4.3.2 Full spectral trends

Labview intensity charts can stack up successive amplitude full spectra. Full spectra are one of the most efficient data processing methods to diagnose vibrations in shaft lines [11].

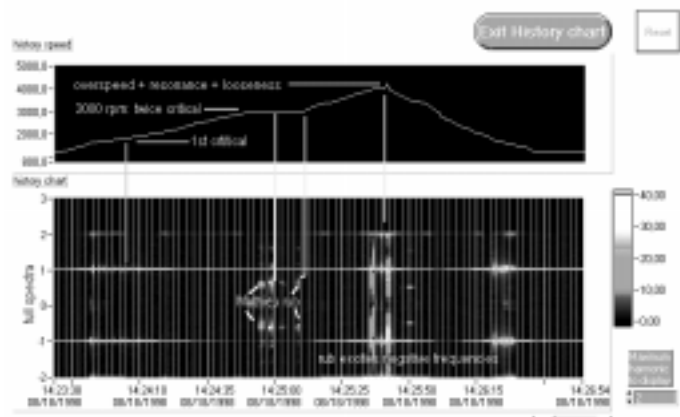


Fig.11. It shows full frequency spectra when crossing two critical speeds at ca 1500 and 4000 rpm. Ordinates range from minus (backward whirl) to plus (forward whirl) the harmonic 2 of the shaft running speed. At double the first critical speed, intermittent soft rub produces vibrations at half the rotational frequency. This is called Mathieu rub. At the second critical speed at ca 4000 rpm the vibrations run counter the shaft rotation since order  $-1$  is dominant. The intensity charts refresh every second in real-time allowing an on-line diagnosis.

### 4.4 A flexible hard-ware

All three applications thus far rely on the same data acquisition card and the same sensors. Therefore, one need not transport cargoes of equipment to the field to play all three acts simultaneously there depending on the problem facing the engineer. Simply provide the vi's on the PC he carries along.

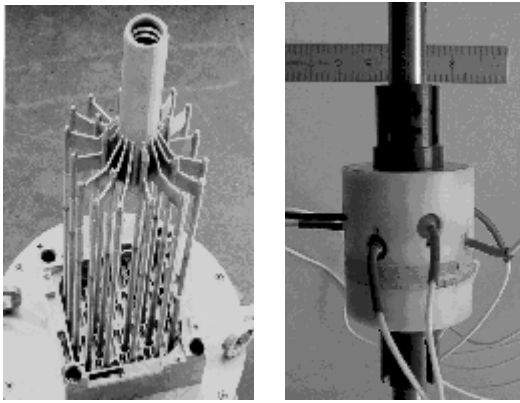


Fig.14. Spider-like descent of fuel rods in Inspection block. Individual rods slide along penetrations in the block, each fitted with an aggregate eddy sensor consisting of an integrated eddy probes and 8 distributed local eddy probes.

### 5.3 Features of the measurement and analysis package

In contrast with other applications, the data acquisition is not implemented in Labview whose purpose here is to streamline the subsequent off-line analysis task from CD-based data for the comfort productivity. The diagnosis mimics heuristic rules based upon signatures from calibrated defects and field practice.

Labview came handy when dialoging with experts while establishing the analysis vi's and tailoring the controls and indicators of the user front panel to their wishes. Zooming on interesting zones of the rod signatures from data files with cursors is a real help

The sheer volume of data to handle required some care in memory usage by Labview. It was the job of a seasoned computer specialist.

### 5.4 The front panel vi

It basically displays the signatures from the 9 eddy probes from an aggregate probe. Sharp transitions in the integrating probe signal a problem, unless it is located at a constructive transition of the rod. Defect positions are retrieved from incremental encoders (topper) monitoring the descent of the rod into the inspection block.

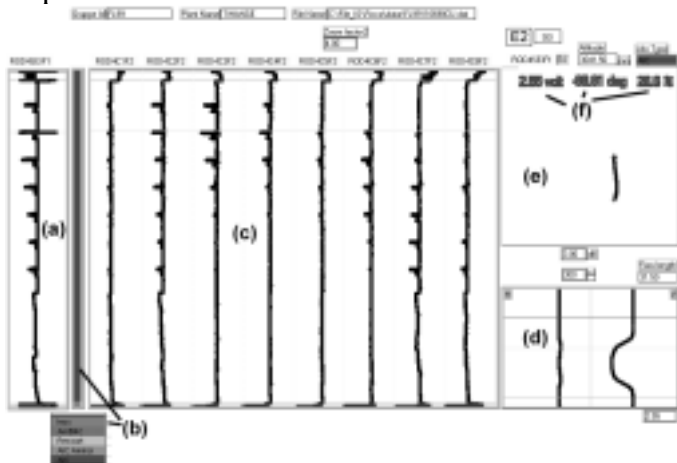


Fig.15. BW Layout of the vi front panel with (a) the overall signature of the integrating probe over the whole rod (b) a

color ramp for the rod height. It is split in several colors depending on the rod construction as shown in the display below. Transitions of the rod nature may cause transient in eddy probes (c) ditto for the 8 distributed probes for wear shape identification (d) zoomed signature of the integrating probes (e) the signature in polar representation (amplitude-phase) normally vertical except in some special cases. (f) a display of the fault severity in % based on calibrated defects.

As another aid to the analyst, a vi panel summarizes the distribution of the response of the 8 local probes at 45° spaced azimuths.

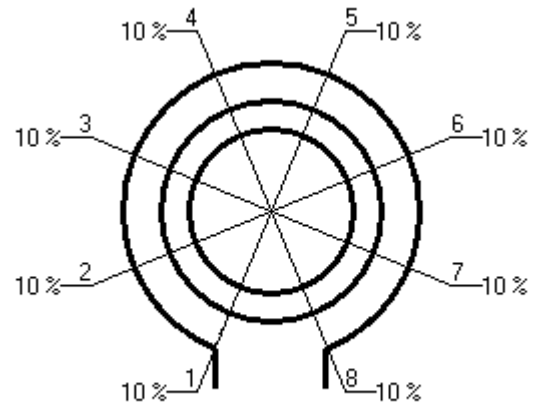


Fig.16. The analyst can also ascertain the type of defect by looking at the transient responses of the eight distributed azimuthal probes. For example, transients that show on several successive local probe signatures point to a C-shaped defect.

### 5.5 Fall-outs

Such a tool greatly reduces the time devoted to the analysis of RCCA inspections, because it was customized to the end user and thus well accepted.

## 6 CONCLUSIONS

Prototyping advanced NDT applications is eased by the advent of tools more intuitive for applications engineers than standard programming techniques.

One of these tools is Labview G-programming. Combined with portable and versatile hardware, it opens the door to field as well as laboratory applications. One need only carry a PC with multiple virtual instruments instead of cargoes of dedicated expensive devices, each one appropriate to troubleshooting a given class of problems. I

Very advanced data processing techniques are made available for the application designer who can make a more knowledgeable use of them than computer specialists and with great comfort. Cepstral techniques to diagnose defects in roller-element bearings, time-frequency spectrograms for gear analyses, order-track multi-channel vibration monitoring are as many witnesses thereof.

Finally, the man-machine interface can be easily prototyped to tailor the virtual instruments to "time-

variable" wishes of end users interactively. This characterizes the last application.

Of course, this was possible with the new PC architectures with fast and large displays, lots of RAMs and fast processors.

## 7 REFERENCES

- [1] Laborelec site: [www.laborelec.be](http://www.laborelec.be)
- [2] National Instruments site: [www.natinst.com](http://www.natinst.com)
- [3] ACME site Germany: [www.acme.de](http://www.acme.de)
- [4] Applied Mechanics Free University Brussels: [www.ulb.ac.be/sam/](http://www.ulb.ac.be/sam/)
- [5] Sturm et al. :Wälzlagerdiagnosen an Maschinen und Anlagen, Verlag TÜV Verein Rheinland, 1986
- [6] P. Eschmann, Hasbargen, Weigand, R. Brandlein: Ball and Roller Bearings : Theory, Design, and Application, Wiley
- [7] L.F. Pau: Failure Diagnosis and Performance Testing Series Control and Systems Theory vol. 11, Marcel Dekker]
- [8] S. Braun: Mechanical Signature Analysis Academic Press, 1986
- [9] Shie Qian, Dapang Chen: Joint Time-Frequency Analysis : Methods and Applications, Prentice Hall, 1996
- [10] J.D. Smith: Gears and their Vibration: A basic approach to understanding gear noise, Marcel Dekker, McMillan, New York, 1983.
- [11] Bently Nevada site: [www.bently.com](http://www.bently.com)
- [12] Project leaders: [pierre.cerckel@laborelec.be](mailto:pierre.cerckel@laborelec.be) (new) and [dirk.degreve@laborelec.be](mailto:dirk.degreve@laborelec.be) (past)